Journal of Power and Energy Engineering, 2023, 11, 1-16
https://www.scirp.org/journal/jpee
ISSN Online: 2327-5901
ISSN Print: 2327-588X

Conjugate Heat Transfer Predictions of Gas Turbine Hot Walls Jets Cooling: Influence of Short Hole Grid Resolutions Using Computational Fluid Dynamics*

Abubakar M. El-Jummah[1,2#], Shehu A. Abdulrahman[1], Alhaji S. Grema[3]

[1]Department of Mechanical Engineering, University of Maiduguri, Maiduguri, Nigeria
[2]Department of Mechanical Engineering, Nigerian Army University Biu, Borno, Nigeria
[3]Department of Chemical Engineering, University of Maiduguri, Maiduguri, Nigeria
Email: #al-jummah@hotmail.com

How to cite this paper: El-Jummah, A.M., Abdulrahman, S.A. and Grema, A.S. (2023) Conjugate Heat Transfer Predictions of Gas Turbine Hot Walls Jets Cooling: Influence of Short Hole Grid Resolutions Using Computational Fluid Dynamics. *Journal of Power and Energy Engineering*, **11**, 1-16.
https://doi.org/10.4236/jpee.2023.1110001

Received: October 11, 2023
Accepted: October 28, 2023
Published: October 31, 2023

Abstract

Short hole investigations relevant to gas turbine (GT) hot walls cooling heat transfer techniques, were carried out using computational fluid dynamics (CFD) combined with conjugate heat transfer (CHT) code. The CFD software are commercial ones: ICEM for grid modelling and ANSYS Fluent for the numerical calculation, where symmetrical application prevails. The CFD CHT predictions were undertaken for Nimonic-75 metal walls with square (152.4 mm) arrays of 10 holes, whereby the lumped heat capacitance method was applied in order to determine the surface average heat transfer coefficient (HTC), h (W/m^2 K) and the dimensionless Nusselt number, Nu. The major parameters considered for the short hole geometries are the pitch to diameter, X/D and length to diameter, L/D ratios and both were varied with range of D values, but X of 15.24 mm and L of 6.35 mm kept constant. Also applied, are variable mass flux, G (kg/s·m^2) and were used in predicting the flow aerodynamics in the short holes. The predictions were for classic thermal entry length into a round hole, as vena contracta, flow separation and reattachment dominates the holes, hence the development of thermal profile through the depth of the GT hot walls. Additionally, the acceleration of the flow along the wall surfaces as it approaches the holes, was a significant part of the overall heat transfer. This was shown to be independent of the hole length, even though the L/D parameter is a critical component to enhanced heat transfer.

*Fluid (air) flow in a short hole with 90˚ entrance edges, resulted into vena contracta effect, which affect the actual flow area of the hole. This research work concentrate on the predictions of heat transfer in the short hole using the combined efforts of CFD and CHT code.

#Corresponding author.

The CFD CHT predictions showed that validation of the HTC h, Nu and pressure loss, ΔP are in better agreement with measured data and within reasonable acceptance. The ΔP agreement signifies that the aerodynamics were predicted correctly, which is also the reason why the HTC expressed per wall hole approach surface area and Nu were better predicted. This illustrates how effective and efficient the wall internal heat transfer cooling is for gas turbine hot wall heat transfer using airflow jets cooling.

Keywords

Lumped Heat Capacitance, Thermal Entry Length, Symmetrical Application, Flow Separation, Flow Reattachment

1. Introduction

Improved wall heat transfer cooling of gas turbine (GT) hot walls: combustor and turbine blades, enhances the efficiency of the GT power generating plant. Is an established fact that the GT combustion temperatures (combustor exit or turbine entry) are well in excess of the melting point of the metal materials [1] [2] of the component walls, hence the needs for better and optimized cooling techniques, as **Figure 1** shows. This advances in providing improvement to the GT power system, is the reason why emission is optimally controlled and the thermal resistance materials are continuously protected. In addition, the cooling air is minimized due the application of effective cooling techniques [3] [4], typically impingement jet cooling (**Figure 1**) using short holes [5] [6], where the cycle thermal efficiency is improved and carbon dioxide (CO_2) and NOx emissions are lowered [6] [7] [8] [9].

Typical GT cooling walls [10] [11] are the instances where a short hole acts as a heat exchanger to cool the target wall or protect it as film shields, hence an efficient system with substantial cooling design mechanisms. This application occurs in either effusion, impingement or combination of both cooling techniques, as the schematic of the experimental rigs of **Figure 2(a)** and **Figure 2(b)** show, where **Figure 2(b)** is meant for future development and experimental procedures. The aerodynamics of short holes involve inlet entry effects [12] that create a region of vena contracta, which generates inlet flow separation and reattachment [3] [6] [13] in the hole which also results into flow development at the hole exit. Significantly, the design variables that are critical to the short hole are the pitch, X to diameter, D and length to D ratios: X/D [9] [14] and L/D [15], which also helps in determining the number of holes per surface area, n (m^{-2}) and the total number of hole, N for the cooling wall. This work enables the use of computational fluid dynamics (CFD) combined with conjugate heat transfer code to better understand flow aerodynamics in the hole and use the results to optimize the design.

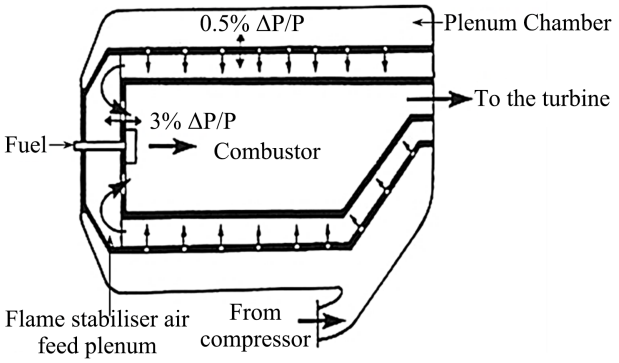

Figure 1. Schematic diagram of a regenerative cooled combustor using short holes as jets.

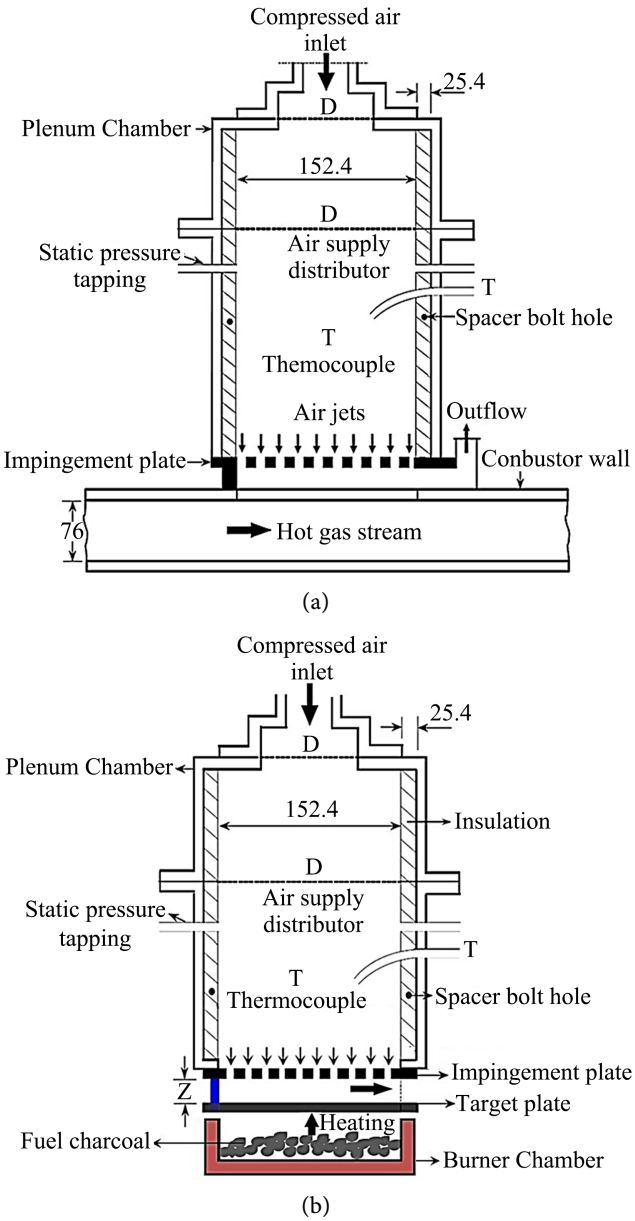

Figure 2. Experimental rig used for validation of the CFD predictions and proposed rig. (a) Hot gas flow heating rig [9] [13]; (b) Coal heating rig.

1.1. Short Hole Aerodynamics

The key experimental parameter that has been shown to be a significant factor in ascertaining that flow aerodynamics are adequately captured in the cooling short holes, is the pressure loss, ΔP (Equation (1)). It provides that if ΔP is successfully predicted, then the hole inlet flow separation and reattachment are also correctly predicted, hence the vena contracta effects [3] [13]. Therefore, work here concentrate on resolving and predicting the hole flow characteristics, in order to compare measured data with CFD predictions. The correctness of the ΔP (Equation (1)), is also the perfection of the flow velocities, turbulence kinetic energy (TKE), k (m^2/s^2) and the heat transfer coefficient (HTC), h ($W/m^2 \cdot K$) [9] [13] [16] [17] [18] [19] [20] as Equations (1) - (5) shows, which this CFD CHT work is expected to reveal. Similar analysis (CFD CHT), can also be applied to other cooling techniques with short holes and 90˚ entrance region.

Work here, predominantly concentrate on the hole in the cooling wall with small thickness, in order to understand the effects of the geometrical design parameters alongside mass flux, G ($kg/s \cdot m^2$). The equivalent of the cooling wall thickness, is the short hole where cooling air as ambient or sea temperatures of 25˚C or 15˚C [5] [7] [21], respectively with a range of inlet velocities are used. This results into the hole Reynolds number, hence the CFD simulation is enabled for the predictions of the flow fields that characterize cooling efficiently [19] [22] [23] [24] [25]. Work here, ignores the impact of the airflow on the impingement target plate and does not consider the flow resolutions in the impingement gap and effects of the reversed flow jets, but the visual outlook will be shown using Equation (5), for a better understanding of its impacts. Worth noting is that the CHT is the influence of combined fluid and solid interactions, whereby conduction inside a solid wall and convection of fluid along the wall surface coexists, as shown in Equation (3). This relationship is based on the wall boundary layer concept where at the surface, energy transfer is only by conduction as fluid motion is at zero velocity with thermal conductivity, k = kf. Hence, Equation 3 is from the combined concepts of heat transfer laws: Fourier's Equation and Newton's law of cooling [6] [26] [27], where fluid thermal effects and temperature differences characterized the HTC.

$$V_j = \frac{G}{\rho A} = \frac{4G}{\pi \rho}\left(\frac{X}{D}\right)^2 = C_d\left(2RT\frac{\Delta P}{P}\right)^{0.5} \tag{1}$$

$$h = \frac{q''}{T_s - T_\infty} \tag{2}$$

$$h = \frac{-k_f\, \partial T/\partial y\big|_{y=0}}{T_w - T_\infty} \tag{3}$$

$$Nu = \frac{hD}{k_f} \tag{4}$$

$$T^* = \frac{T - T_\infty}{T_w - T_\infty} \tag{5}$$

1.2. Cooling Heat Transfer and Nusselt Number

Protecting the life of the GT hot walls, significantly satisfy the requirements for high power output and low fuel consumption, which are better achieved using cooling techniques [1] [2]. The GT cycle thermal efficiency, which is controlled by the turbine entry temperature (>2800 K for aero engines [28] in the near future), is also a significant factor that must be adequately managed. This is in order to keep the walls of the GT combustor and turbine blades within a safe operating temperature and would not be above the melting point of the metal walls. To effectively cool the walls, the geometrical design and heat transfer analysis must be correctly carried out, hence Equations (2) and (4) are applied in the CFD code in order to conduct the predictions. With metallurgical limitations of the metal materials, cooling the walls of the GT component, is a reliable method of protecting the GT engine from the hot gas core flow or stream, as **Figure 2(a)** show.

Reliably, GT hot metal walls cooling helps in controlling [15] [29] [30] [31] the effects of increased turbine inlet temperature alongside the associated pollutant emissions [32] [33] that also affects the air mass flow rate, as in **Figure 3**. Optimizing the GT cooling design in order to overcome material deterioration and minimized emissions, the solution is the application of CFD CHT tool. The dimensional wall convective cooling heat transfer coefficient (HTC), h (W/m^2·K) of Equation (2), is defined in the CFD code to ascertain cooling effectiveness, which is normalized as dimensionless Nusselt number, Nu and is based on the geometry and thermal effects, as in Equation 4. Both Equations (2) and (4) are used in the present CFD research work, to validate the CFD predictions. Also the temperature differences that indicates influence of heat transfer are normalized in Equation (5), which is in order to show the reversed heating of air jets will be revealed here, as this is rarely shown experimentally.

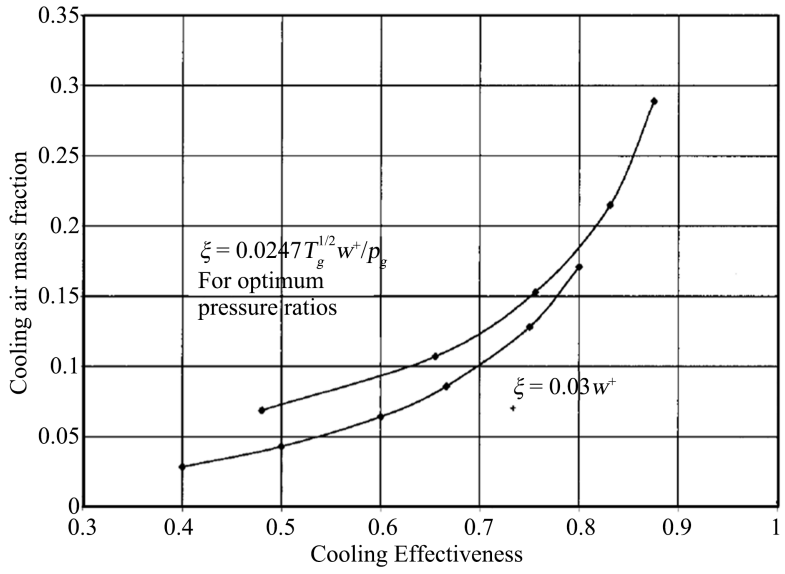

Figure 3. Expression for the approximation of cooling air flow mass fraction [28].

2. CFD Methodology

2.1. Grid Generation

Grid sensitivity test using ICEM meshing combined with ANSYS Fluent tools was previously carried out by El-jummah *et al.* [34], which work here also adopts. This work implored the same grid refinement techniques in the hole with grid size (~60 cells/plane) varying based on X/D or G values using hexahedral structured grid [9] [27] [35] [36] [37]. **Table 1** show the parameters that were used to transformed the computational diagram of **Figure 4** into the grid modelled geometry of **Figure 5**, where the half short hole with smooth surface was also shown. Experimentally [3], the hole wall typical of Nimonic-75 material [38] [39], cannot be smooth and is based on roughness effects that is due to certain inaccuracies caused by the porosity of material or drilling equipment. **Figure 4** show that application of symmetry was imposed at the centre line of hole and plane between rows of 10 × 10 holes, which is a replica of the experimental rig shown in **Figure 2**. **Table 2** shows that the percentage of grid size in the holes with varied X/D, indicates that higher X/D gives larger percentage of grids in the holes. Also worth noting is that decreasing G decreases the number of cells in the hole, hence for every X/D and with changes in G, grid size is also altered accordingly.

Table 1. Geometrical parameters for the computational modelled grid array of holes.

Parameters	X/D			
	11.04	**6.99**	**6.54**	**4.66**
D **(mm)**	1.38	1.42	2.33	3.27
L **(mm)**	6.35	6.35	6.35	6.35
Z **(mm)**	10.00	10.00	10.00	10.00
L/D	4.60	4.47	2.73	1.94
Z/D	7.25	7.04	4.29	3.06
n **(%)**	4306	4306	4306	4306

Z/D is important but is not part of this work and is meant to show that the exit air is also flown out.

Table 2. Grid size and Y^+ values applied to the modelled short holes.

X/D	Grid Size		y^+
	Air Jet Cooling Holes (%)	**Total in Geometry**	
11.04	7.09	2.08×10^6	44.8
6.99	6.76	1.87×10^6	41.5
6.54	6.62	1.77×10^6	39.2
4.66	6.13	1.27×10^6	35.6

The Table excludes other parts of the geometry, as work here only deals with short holes.

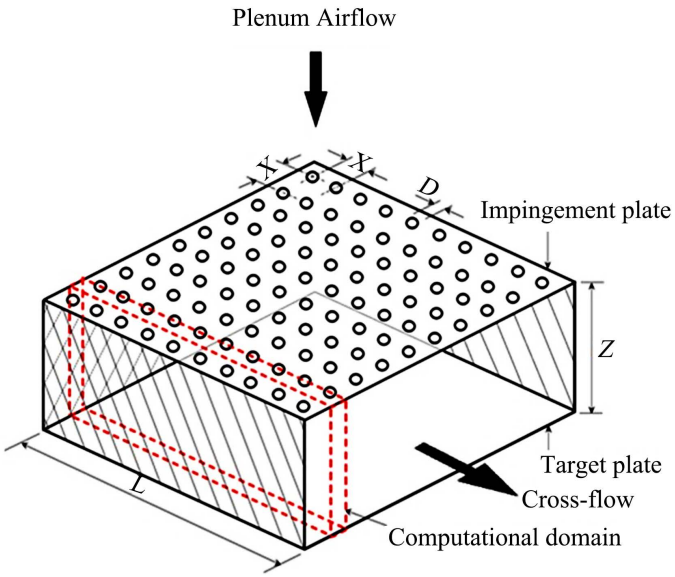

Figure 4. Computational flow domain and symmetrical set up.

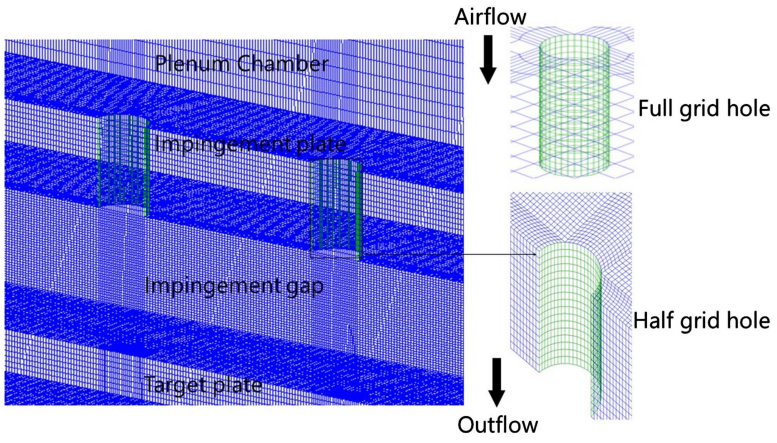

Figure 5. Short holes computational modelled grid applicable to GT cooling technique.

2.2. Model Grid Computation

ANSYS Fluent CFD code is the numerical software used in this work and the calculations (using flow parameters in **Table 3**) for all the geometries modelled, were carried out using standard wall function approach and standard k - ε turbulence model. The range of y^+ values increases [6] [9] with increased X/D and G of 1.93 kg/s·m^2 (**Table 2**), which was based on the uniformity of the cells down through the holes, it also indicates resolution of air flow fields in the holes. The values of the y$^+$ (operates within near wall law $30 < y^+ < 300$) [40] [41] [42] in all cases have been shown by El-jummah *et al.* [9] [20] to captured high or low Reynolds number flow approach in the short holes, hence L/D effects [15]. The initial and boundary conditions (BC) imposed includes: fixed inlet coolant and hot-side temperatures, T_∞ of 288˚C and 353˚C, respectively, density, ρ of 1.225 kg/m^3, velocity inlet (G/ρ)/outflow, walls (hole, sides, coupled thermal and temperature) symmetry. Turbulence intensity of ~5% calculated from the plenum

Table 3. Computational flow parameters used for the CFD predictions.

Parameters	Air Mass Flux, G (kg/s m²), X/D of 4.66 and D of 3.27 mm				
	1.93	**1.48**	**1.08**	**0.71**	**0.35**
V_j (m/s)	43.4	33.5	24.3	16.0	7.7
Re_h	9680	7440	5400	3560	1650
T_∞ (K)	288	288	288	288	288
ρ (kg/m³)	1.225	1.225	1.225	1.255	1.225

Target wall temperature applied in this work is 353 K.

inlet Reynolds number and hydraulic diameter. The criteria that were sets for convergence includes: 10^{-5} for continuity, 10^{-8} for energy and 10^{-7} for k, ε, ω and momentum (x, y and z velocities), respectively. Iterations were run and converges using steady state solutions at flow time ~0.05 s and in order to stabilized the computations, transient simulations were also carried out. An industrial and upgraded generation type of high performance computer (HPC) was used, which is in order to adequately calculate regions of flow and heat transfer with large number of grids and regions with refined grids and cell growth downstream the hole exits.

3. Computational Results and Discussions

Table 3 shows the flow parameters that were imposed as initial and boundary conditions used for each numerical calculations carried out here, which is for X/D of 4.66. Similar Tables for other X/D that were shown in Table 1, are also available but not shown here, implying that for each G assigned to an X/D shown in Table 3 is one grid geometry and computational effort. Also, the size of the grid cell depends on the values of X/D and G, if X/D and G are large, the number of cells is also high, but with large X/D and small G the grid size is reduced but lower than that with smaller values of X/D and G.

3.1. Short Hole Flow Visualization and Characterization

Figure 6 and Figure 7 show typical description of flows as depicted by work of Cho and Goldstein [3] of Figure 6 that vena contracta effects, results into flow separation and reattachment, which also increases the flow velocity with flow reduced area. Their work was compared with this CFD predictions in Figure 6, it reveals that the regions that were described by Cho and Goldstein [3] are correctly predicted by the velocity pathlines and TKE, k results. It shows from the TKE predictions that flow reattachment also creates vortices that possibly have consequential effects on the air mass flow, G for $X/D = 4.66$, as in Figure 7. Figure 7 indicates that if G is less than 0.35 kg/s m², the effects of the contracta could affect the reattaching flow and increases the downstream air jets velocity, while other Gs are not affected as the flows are within the vena contracta regions, implying that the ΔP is expected to be valid, as in Figure 8. This implies

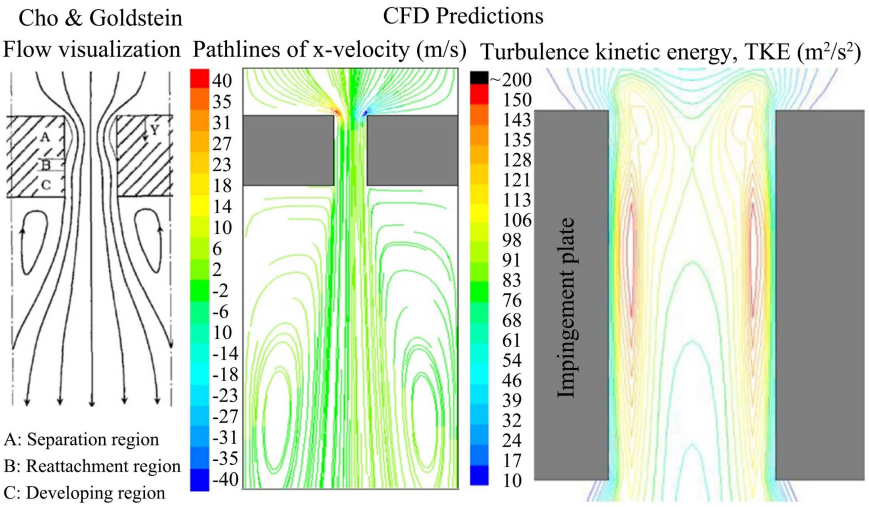

Figure 6. Comparison of literature based visualization of flow with CFD predicted flow.

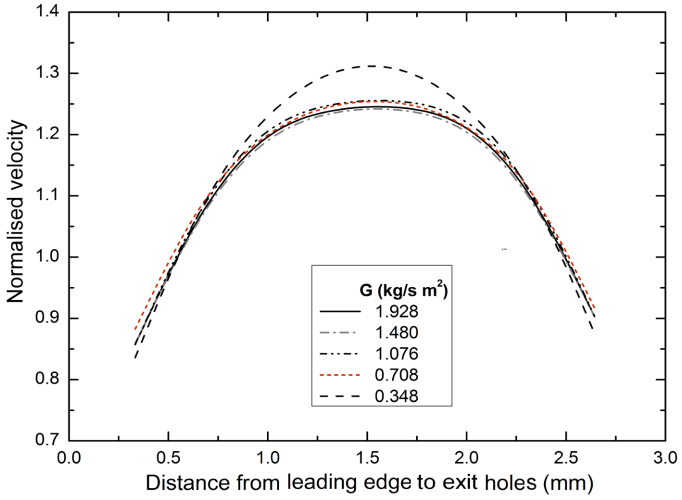

Figure 7. CFD predicted hole flow velocity normalized to the mean velocity for varied *G*.

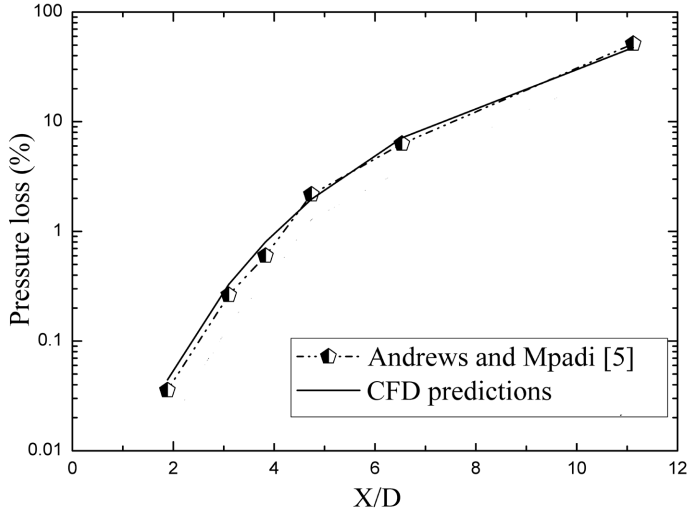

Figure 8. Comparison of CFD predicted pressure loss with experimental data.

that the CFD predictions with the application of the refined hexahedral structured grid, wall function and standard k - ε turbulence model, captured well the flow aerodynamics in the hole and the use of high performance computer (HPC) is adequate for the CFD calculations.

3.2. Validation of the CFD Predictions

Comparison of measured data and CFD predictions were made in **Figure 8** and **Figure 9**, whereby pressure loss and heat transfer coefficient for the hole wall boundaries are correctly predicted. **Figure 8** shows that ΔP increases with increased X/D and there is perfect agreement with work by Andrews and Mpadi [5], as both the geometrical and flow parameters are similar to that simulated in this work. Also predicted correctly with the experimental data [5] and within the 10% experimental error bar, is the surface average HTC of **Figure 9**. It shows similar trend with that predicted in **Figure 8**, which indicates that ΔP influences HTC, hence the aerodynamics in the short holes that captured the flow separation and reattachment (**Figure 6** and **Figure 10**).

Figure 11 is the comparison of Nusselts number per measured data of work by Mills [12] with this CFD prediction. It shows reasonable agreement and with insufficient influence on L/D. The disparity in agreement could be based on the fact that the experimental parameters vary with the computational one but are closely similar and the differences are insignificant, hence comparisons are possible. **Figure 8**, **Figure 9** and **Figure 11** show that the experimental results validate the CFD predictions, which implies that the use of the present CFD code and techniques are adequate in optimising the design procedures used here. **Figure 10** shows that conjugate heat transfer can also be combined with CFD tools in order to predict the complex mechanisms in the short hole that experimentally are either not possible or are costly.

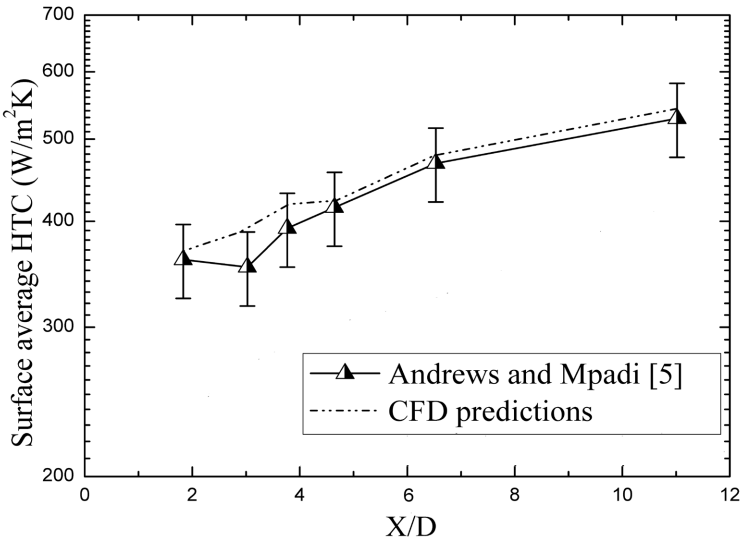

Figure 9. Comparison of CFD prediction with literature based heat transfer measured data.

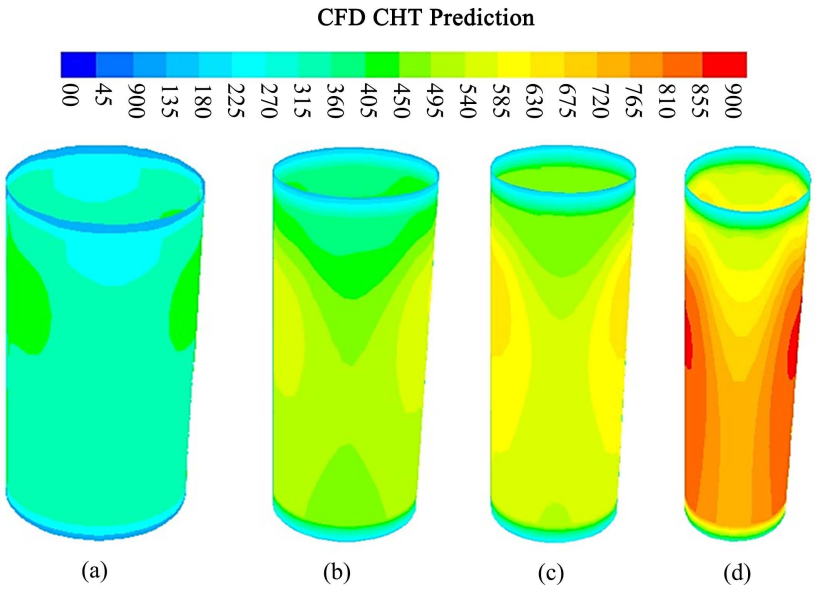

Figure 10. Circular Short holes surface average heat transfer coefficient, h (W/m²·K). (a) $X/D = 4.66$; (b) $X/D = 6.54$; (c) $X/D = 6.99$; (d) $X/D = 11.04$.

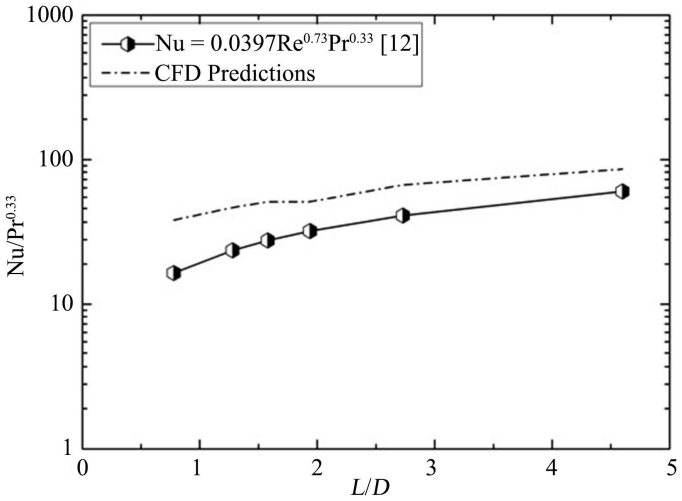

Figure 11. Comparison of predicted surface average Nusselt number with measured data.

3.3. Conjugate Heat Transfer

Figure 10 shows that the predicted heat transfer is clearly the influenced of the TKE aerodynamics prediction of Figure 12, with a similar trend of prediction for the Nusselts number result in Figure 12. This further demonstrates the predicted results shown in Figure 6 and the consequences associated with aerodynamics, whereby largely the Reynolds number, Re in Table 3 are turbulence in nature and hence resulted into jets flow. The used of Equation (5) (T^*) reveals that the exit hole sides are associated with reversed air jets flow as in Figure 12, which also affects the conjugate heat transfer in the hole wall surfaces and is the reason why high X/D with high Re of Figure 10 gave high transfer. Also shown in Figure 13 is T^*, which indicates that upstream holes extract heat higher with

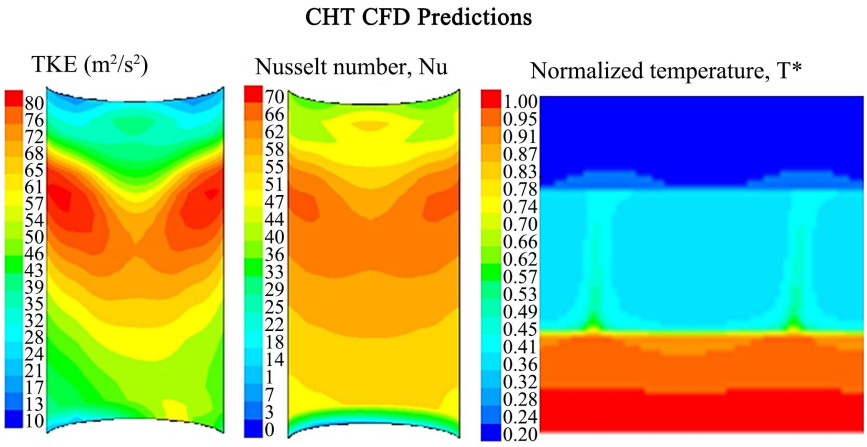

Figure 12. Influence of vena contracta in circular short holes and cooling air jet flows.

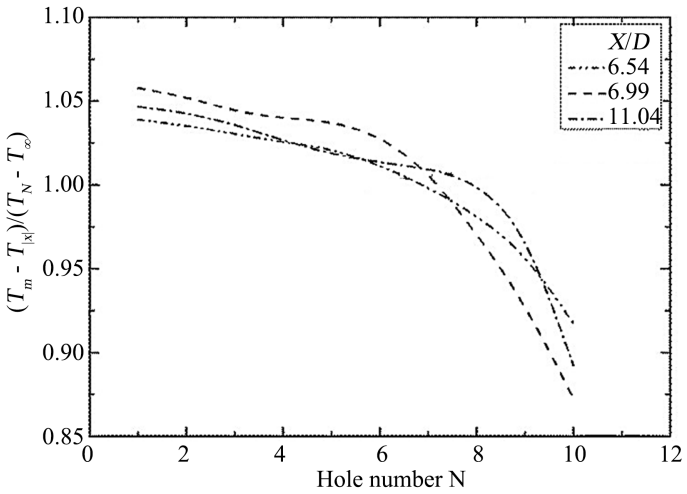

Figure 13. X^2 average hole surface thermal gradient shown as normalized temperature.

X/*D*, while downstream holes gave lower heat transfer as a result of crossflow effects [9] [13] [19] [20].

4. Conclusions

Applications of jet cooling using the combination of conjugate heat transfer and computational fluid dynamics, were achieved and validated with experimental data. This is to further optimize the design procedures that apply to gas turbine cooling systems.

The use of conjugate heat transfer has revealed that enhancing heat transfer cooling depends critically on the aerodynamics as well as the pressure loss. If the aerodynamics are well captured, pressure loss will be correctly predicted which has significant effects on the characterization of the heat transfer on the gas turbine hot walls.

The CHT CFD predictions showed that gas turbine cooling techniques are better modified, upgraded and developed using CFD codes. It further reveals that the use of numerical tools reduces cost as a larger number of computation-

ally modelled grids could be generated within the framework of high performance computer systems and licensed software packages.

5. Recommendations

Future work will be looking at experimental facilities that are expected to give higher heat flux with a thermal gradient of the material falling within its standard limitations. Also to at include considering grid types and turbulence models.

Acknowledgements

The Authors acknowledged the IBR support for a research grant from the Tertiary Education Trust Fund (TETFund), Nigeria and nomination by University of Maiduguri, Borno State, Nigeria.

Conflicts of Interest

The authors declare no conflicts of interest regarding the publication of this paper.

References

[1] Brooks, F.J. (2010) GE Gas Turbine Performance Characteristics. GE Power Systems, Schenectady.

[2] Eisako, I., Ikuo, O. and Keizo, T. (2009) Development of Key Technologies for the Next Generation 1700˚C-Class Gas Turbine. ASME Turbo Expo: Power for Land, Sea and Air, GT2009-59783.

[3] Cho, H.H. and Goldstein, R.J. (1997) Total-Coverage Discrete Hole Wall Cooling. *Journal of Turbomachinery*, **119**, 320-329. https://doi.org/10.1115/1.2841115

[4] Cho, H.H., Jabbari, M.Y. and Goldstein, R.J. (1997) Experimental Mass (Heat) Transfer in and Near a Circular Hole in a Flat Plate. *International Journal of Heat and Mass Transfer*, **40**, 2431-2443. https://doi.org/10.1016/S0017-9310(96)00270-0

[5] Andrews, G.E. and Mpadi, M.C. (1984) Full-Coverage Discrete Hole Wall Cooling: Discharge Coefficients. *Journal of Engineering for Gas Turbines and Power*, **106**, 183-192. https://doi.org/10.1115/1.3239533

[6] El-Jummah, A.M., Andrews, G.E. and Staggs, J.E.J. (2015) Conjugate Heat Transfer CFD Predictions of Metal Walls with Arrays of Short Holes as Used in Impingement and Effusion Cooling. *Proceedings of the* 11*th Japanese International Gas Turbine Congress* 2015, Tokyo, 15-20 November 2015, 1495-1503.

[7] Andrews, G.E., Matt Lazim, T.B. and Mpadi, M.C. (2005) Low NOx Axial Swirler with Fuel Injection into the Downstream Dump Expansion Shear Layer. *Journal of the Energy Institute*, **78**, 172-184. https://doi.org/10.1179/174602205X68298

[8] Andrews, G.E., Wang, J. and Abdul Husain, R.A.A. (2011) CFD Predictions of the Aerodynamics and Heat Transfer from Arrays of Impingement Jets with Crossflow. GTSJ International Gas Turbine Congress, IGTC-0141.

[9] El-Jummah, A.M., Abdul Husain, R.A.A., Andrews, G.E. and Staggs, J.E.J. (2014) Conjugate Heat Transfer Computational Fluid Dynamic Predictions of Impingement Heat Transfer: The Influence of Hole Pitch to Diameter Ratio X/D at Constant Impingement Gap Z. *Journal of Turbomachinery*, **136**, Article ID: 121002. https://doi.org/10.1115/1.4028232

[10] Andrews, G.E. and Hussain, C.I. (1984) Impingement Cooling of Gas Turbine Components. *High Temperature Technology*, **2**, 99-106. https://doi.org/10.1080/02619180.1982.11753248

[11] Facchini, B. and Surace, M. (2006) Impingement Cooling for Modern Combustors: Experimental Analysis of Heat Transfer and Effectiveness. *Experiments in Fluids*, **40**, 601-611. https://doi.org/10.1007/s00348-005-0100-y

[12] Mills, A.F. (1962) Experimental Investigation of Turbulent Heat Transfer in the Entrance Region of a Circular Conduit. *Journal of Mechanical Engineering Science*, **4**, 63-77. https://doi.org/10.1243/JMES_JOUR_1962_004_010_02

[13] El-Jummah, A.M., Abdul Husain, R.A.A., Andrews, G.E. and Staggs, J.E.J. (2013) Conjugate Heat Transfer CFD Predictions of the Surface Averaged Impingement Heat Transfer Coefficients for Impingement Cooling with Backside Cross-Flow. *ASME* 2013 *International Mechanical Engineering Congress and Exposition*, San Diego, 15-21 November 2013, 1-14. https://doi.org/10.1115/IMECE2013-63580

[14] Andrews, G.E., Asere, A.A., Hussain, C.I. and Mkpadi, M.C. (1985) Full Coverage Impingement Heat Transfer: The Variation in Pitch to Diameter Ratio at a Constant Gap. 65*th Symposium*, *Heat Transfer and Cooling in Gas Turbines*. Bergen, 6-10 May 1985, 1-13.

[15] Andrews, G.E., Bazdidi-Tehrani, F., Hussain, C.I. and Pearson, J.P. (1991) Small Diameter Film Cooling Hole Heat Transfer: The Influence of the Hole Length. *Proceedings of the ASME* 1991 *International Gas Turbine and Aeroengine Congress and Exposition*, Orlando, 3-6 June 1991, V004T09A021. https://doi.org/10.1115/91-GT-344

[16] El-Jummah, A.M., Abdul Husain, R.A.A., Andrews, G.E. and Staggs, J.E.J. (2014) Conjugate Heat Transfer CFD Predictions of Impingement Heat Transfer: Influence of the Number of Holes for a Constant Pitch to Diameter Ratio X/D. *Proceedings of the ASME Turbo Expo* 2014: *Turbine Technical Conference and Exposition*, Düsseldorf, 16-20 June 2014, V05AT11A004. https://doi.org/10.1115/GT2014-25268

[17] El-Jummah, A.M., Mukhtar, U.A. and Adam, M.K. (2016) Computational Fluid Dynamic Procedures for Grid Generation and Solution Induced Cooling Applied to Gas Turbine Hot Walls (MSS 1025). *Annals of Borno Journals*, **XXVI**, 95-112.

[18] El-Jummah, A.M., Abdul Husain, R.A.A., Andrews, G.E. and Staggs, J.E.J. (2017) Impingement/Effusion Cooling Wall Heat Transfer: Reduced Number of Impingement Jet Holes Relative to the Effusion Holes. *Proceedings of the ASME Turbo Expo* 2017: *Turbomachinery Technical Conference and Exposition*, Charlotte, 26-30 June 2017, V05CT17A005. https://doi.org/10.1115/GT2017-63494

[19] El-Jummah, A.M., Andrews, G.E. and Staggs, J.E.J. (2013) Conjugate Heat Transfer CFD Predictions of Impingement Jet Array Flat Wall Cooling Aerodynamics with Single Sided Flow Exit. *Proceedings of the ASME Turbo Expo* 2013: *Turbine Technical Conference and Exposition*, San Antonio, 3-7 June 2013, V03BT11A015. https://doi.org/10.1115/GT2013-95343

[20] El-Jummah, A.M., Andrews, G.E. and Staggs, J.E.J. (2013) Conjugate Heat Transfer CFD Predictions of the Influence of the Impingement Gap on the Effect of Crossflow. *Proceedings of the ASME* 2013 *Heat Transfer Summer Conference Collocated with the ASME* 2013 7*th International Conference on Energy Sustainability and the ASME* 2013 11*th International Conference on Fuel Cell Science*, *Engineering and Technology*, Minneapolis, 14-19 July 2013, V003T08A006. https://doi.org/10.1115/HT2013-17180

[21] Andrews, G.E. and Kim, M.N. (2001) The Influence of Film Cooling on Emissions

of a Low NOx Radial Swirler Gas Turbine Combustor. *Proceedings of the ASME Turbo Expo* 2001: *Power for Land, Sea, and Air*, New Orleans, 4-7 June 2001, V002T02A038. https://doi.org/10.1115/2001-GT-0071

[22] Sharif, M.A.R. and Mothe, K.K. (2010) Parametric Study of Turbulent Slot-Jet Impingement Heat Transfer from Concave Cylindrical Surfaces. *International Journal of Thermal Sciences*, **49**, 428-442. https://doi.org/10.1016/j.ijthermalsci.2009.07.017

[23] Wang, X., Liu, R., Bai, X. and Yao, J. (2011) Numerical Study on Flow and Heat Transfer Characteristics of Jet Impingement. *Proceedings of the ASME* 2011 *Turbo Expo*: *Turbine Technical Conference and Exposition*, British Columbia, 6-10 June 2011, 1155-1164. https://doi.org/10.1115/GT2011-45287

[24] Hong, S.K., Rhee, D.H. and Cho, H.H. (2007) Effects of Fin Shapes and Arrangements on Heat Transfer for Impingement/Effusion Cooling with Crossflow. *Journal of Heat and Mass Transfer*, **129**, 1697-1707. https://doi.org/10.1115/1.2767727

[25] Cho, H.H., Rhee, D.H. and Goldstein, R.J. (2008) Effects of Hole Arrangements on Local Heat/Mass Transfer for Impingement/Effusion Cooling With Small Hole Spacing. *Journal of Turbomachinery*, **130**, Article ID: 041003. https://doi.org/10.1115/1.2812325

[26] Incropera, F.P., Dewitt, D.P., Bergman, T.L. and Lavine, A.S. (2007) Fundamentals of Heat and Mass Transfer. John Wiley & Sons, Hoboken.

[27] El-Jummah, A.M., Andrews, G.E. and Staggs, J.E.J. (2015) CHT/CFD Predictions of Impingement Cooling with Four Sided Flow Exit. *Proceedings of the ASME Turbo Expo* 2015: *Turbine Technical Conference and Exposition*, Montreal, 15-19 June 2015, V05AT10A004. https://doi.org/10.1115/GT2015-42256

[28] Horlock, J.H., Watson, D.T. and Jones, T.V. (2001) Limitations on Gas Turbine Performance Imposed by Large Turbine Cooling Flows. *Journal of Engineering for Gas Turbines and Power*, **123**, 487-494. https://doi.org/10.1115/1.1373398

[29] Bailey, J.C., Intile, J., Fric, T.F., Tolpadi, A.K., Nirmalan, N.V. and Bunker, R.S. (2003) Experimental and Numerical Study of Heat Transfer in a Gas Turbine Combustor Liner. Trans. *Journal of Engineering for Gas Turbines and Power*, **125**, 994-1002. https://doi.org/10.1115/1.1615256

[30] Arthur, H.L. and Dilip, R.B. (2010) Gas Turbine Combustion. 3rd Edition, CRC Press, New York.

[31] Andrews, G.E., Alikhanizadeh, M., Asere, A.A., Hussain, C.I., Koshkbar Azari, M.S. and Mpadi, M.C. (1986) Small Diameter Film Cooling Holes: Wall Convective Heat Transfer. *Journal of Turbomachinery*, **108**, 283-289. https://doi.org/10.1115/1.3262049

[32] Andrews, G.E., Alkabie, H.S., Abdul Hussain, U.S. and Abdul Aziz, M. (1993) Ultra Low NOx Ultra Lean Gas Turbine Primary Zones with Liquid Fuels. *Proceeding* 536, 81*st Symposium of the Proportion and Energetics Panel of Fuels and Combustion Technology for Advanced Aircraft Engines*, Fiuggi, 10-14 May 1993, 1-14.

[33] Kano, K., Matsuzaki, H., Aoyama, K., Aoki, S. and Mandai, S. (1991) Development Study of 1500°C Class High Temperature Gas Turbine. *Proceedings of the ASME* 1991 *International Gas Turbine and Aeroengine Congress and Exposition*, Orlando, 3-6 June 1991, V004T10A015. https://doi.org/10.1115/91-GT-297

[34] El-Jummah, A.M., Abdul Husain, R.A.A., Andrews, G.E. and Staggs, J.E.J. (2013) Conjugate Heat Transfer CFD Predictions of the Surface Averaged Impingement Heat Transfer Coefficients for Impingement Cooling with Backside Cross-Flow. *Proceedings of the ASME* 2013 *International Mechanical Engineering Congress and Exposition*, San Diego, 15-21 November 2013, V08BT09A059.

https://doi.org/10.1115/IMECE2013-63580

[35] El-Jummah, A.M., Andrews, G.E. and Staggs, J.E.J. (2016) Impingement Jet Cooling with Ribs and Pin Fin Obstacles in Co-Flow Configurations: Conjugate Heat Transfer Computational Fluid Dynamic Predictions. *Proceedings of the ASME Turbo Expo* 2016: *Turbomachinery Technical Conference and Exposition*, Seoul, 13-17 June 2016, V05AT10A006. https://doi.org/10.1115/GT2016-57021

[36] El-Jummah, A.M., Andrews, G.E., and Staggs, J.E.J. (2018) Enhancement of Impingement Heat Transfer with the Crossflow Normal to Ribs and Pins between Each Row of Holes. *ASME Turbo Expo* 2018: *Turbomachinery Technical Conference and Exposition*, Oslo, 11-15 June 2018, 1-13. https://doi.org/10.1115/GT2018-76969

[37] El-Jummah, A.M., Andrews, G.E. and Staggs, J.E.J. (2019) Predictions of Impingement Heat Transfer with Dimples, Pin-Fins and Zig-Zag Rib Obstacles: Conjugate Heat Transfer Computational Fluid Dynamics Predictions. *Proceedings of the ASME Turbo Expo* 2019: *Turbomachinery Technical Conference and Exposition*, Phoenix, 17-21 June 2019, V05AT10A003. https://doi.org/10.1115/GT2019-90730

[38] Andrews, G.E., Durance, J., Hussain, C.I. and Ojobor, S.N. (1987) Full Coverage Impingement Heat Transfer: Influence of the Number of Holes. *Journal of Turbomachinery*, **109**, 557-563. https://doi.org/10.1115/1.3262148

[39] Andrews, G.E., Asere, A.A., Hussain, C.I. and Mkpadi, M.C. (1985) Transpiration and Impingement/Effusion Cooling of Gas Turbine Combustion Chambers. *ISABE and AIAA 7th Propulsion Joint Specialist Conference*, Monterey, 8-11 July 1985, 794-803.

[40] Ariff, M., Salim, S.M. and Cheah, S.C. (2009) Wall Y^+ Approach for Dealing with Turbulent Flow over a Surface Mounted Cube: Part 1—Low Reynolds Number. *Proceedings of Seventh International Conference on CFD in the Minerals and Process Industries*, Melbourne, 9-11 December 2009, 1-6.

[41] Ariff, M., Salim, S.M. and Cheah, S.C. (2009) Wall Y^+ Approach for Dealing with Turbulent Flow over a Surface Mounted Cube: Part 2—High Reynolds Number. *Proceedings of Seventh International Conference on CFD in the Minerals and Process Industries*, Melbourne, 9-11 December 2009, 1-6.

[42] El-Jummah, A.M. (2015) Impingement and Impingement/Effusion Cooling of Gas Turbine Components: Conjugate Heat Transfer Predictions. Ph.D. Thesis, University of Leeds, Leeds.